# Nonlinear Marangoni waves in multilayer systems

Igor L. Kliakhandler,[1] Alexander A. Nepomnyashchy,[2] Ilya B. Simanovskii,[2] and Michael A. Zaks[3]
[1]*School of Mathematics, Tel-Aviv University, Tel-Aviv 69978, Israel*
[2]*Department of Mathematics and Minerva Center for Nonlinear Physics of Complex Systems, Technion–Israel Institute of Technology, 32000 Haifa, Israel*
[3]*Department of Nonlinear Dynamics, Institute of Physics, Potsdam University, D-14415, Potsdam, Germany*
(Received 11 June 1998)

The nonlinear theory of long Marangoni waves in systems with two interfaces is developed by means of asymptotic expansions. The self-consistent three-layer approach is used. In the case where the thickness of one of the layers is small, the system of coupled equations governing the deformations of both interfaces has been derived. Traveling wave solutions of this system are investigated analytically and numerically.
[S1063-651X(98)13510-9]

PACS number(s): 47.20.Dr, 47.54.+r, 03.40.Kf, 47.52.+j

## I. INTRODUCTION

It is well known that the thermocapillary effect (dependence of the surface tension on the temperature) in a liquid layer heated from below can lead to the onset of two kinds of instabilities. First, there exists the *short-wavelength* Marangoni instability generating hexagonal cells [1,2], which can be described by means of coupled Ginzburg-Landau equations [3]. The second type of instability is connected with the *long-wavelength* deformations of the interface [4,5]. The deformational Marangoni instability, which prevails in the case of thin liquid layers or under microgravity conditions, has been observed recently by VanHook *et al.* [6,7] and studied numerically by Krishnamoorthy *et al.* [8].

The evolution of the finite-amplitude long-wavelength surface deformations is governed by the strongly nonlinear equation derived by Davis [9,10]. A simplified weakly nonlinear version of this equation was considered by Funada [11] and Pukhnachev [12]. Numerical simulations of both strongly and weakly nonlinear equations show that unlike the short-wave cellular instability, the long-wavelength deformational instability is not saturable and leads to a blowup of solutions. The experiments [6] justify this prediction, showing the appearance of a dry spot.

The absence of the saturation of the long-wavelength instability may be explained qualitatively in the following way. In the framework of the usual *one-layer* approach, when any processes in the adjacent gas phase are ignored, the critical temperature difference generating the instability is proportional to the squared local thickness of the liquid layer (because the critical Marangoni number is proportional to the Galileo number [5]). Hence the instability is enhanced in the regions where the thickness decreases.

It should be noted, however, that the dependence of the critical temperature difference on the thickness of the liquid layer may be *nonmonotonic* if the phenomena in both liquid and gas layers are taken into account (in the framework of the *two-layer* approach [13]). If the ratio of the thicknesses of liquid and gas layers corresponds to the minimal value of the critical temperature difference, both the increase and the decrease of the local liquid layer thickness weaken the instability. For the latter case, the existence of a stationary relief of the interface is predicted [14].

Recently, a different direction, the investigation of the thermocapillary convection in systems with *two interfaces*, was conceived [15–24]. The interest to such systems was caused by various technical applications, including the liquid encapsulation crystal growth technique [22], emulsified liquid membrane separation techniques [25], and droplet-droplet coalescence processes [26]. It was shown that the coupling between long-wave deformations of two interfaces may lead to a different type of long-wavelength oscillatory instability with an unusual dispersion relation $\omega \sim k^2$ between the frequency $\omega$ and the wave number $k$ [23].

In the present paper we develop the nonlinear theory of long Marangoni waves in systems with two interfaces. The investigation is implemented in the self-consistent three-layer approach. We concentrate on the analytically tractable case, where the thickness of one of the layers is small. The mathematical formulation of the problem is described in Sec. II. In Sec. III we derive the system of amplitude equations governing the evolution of deformations of interfaces. Section IV is devoted to the analytical and numerical investigation of traveling wave solutions. The interaction between traveling waves moving in different directions is considered as well. The results of direct numerical simulations of waves described by the amplitude equations are presented in Sec. V. The concluding remarks are given in Sec. VI.

## II. FORMULATION OF THE PROBLEM

Let the space between two rigid horizontal plates be filled by three immiscible fluids with different physical properties


FIG. 1. Side view of the three-layer configuration.

 

(see Fig. 1). The equilibrium thicknesses of the layers are $a_i$, $i=1,2,3$. The deformable interfaces are described by equations $z=h(x,y,t)$ and $z=-a_2+h_*(x,y,t)$. The $i$th fluid has density $\rho_i$, kinematic viscosity $\nu_i$, dynamic viscosity $\eta_i=\rho_i\nu_i$, heat diffusivity $\chi_i$, and heat conductivity $\kappa_i$. The surface tension coefficients on the upper and lower interfaces $\sigma$ and $\sigma_*$ are linear functions of temperature $T$: $\sigma=\sigma_0-\alpha T$ and $\sigma_*=\sigma_{*0}-\alpha_* T$. The acceleration due to gravity is $g$. We do not take into account buoyancy effects, which are negligible in the case of thin layers or under microgravity conditions.

The horizontal plates are kept at different constant temperatures. The temperature difference can be positive or negative and the overall temperature drop is $\theta$. Let us define

$$\rho=\frac{\rho_1}{\rho_2},\quad \nu=\frac{\nu_1}{\nu_2},\quad \eta=\frac{\eta_1}{\eta_2}=\rho\nu,\quad \chi=\frac{\chi_1}{\chi_2},$$

$$\kappa=\frac{\kappa_1}{\kappa_2},\quad a=\frac{a_2}{a_1},\quad \rho_*=\frac{\rho_1}{\rho_3},\quad \nu_*=\frac{\nu_1}{\nu_3},$$

$$\eta_*=\frac{\eta_1}{\eta_3}=\rho_*\nu_*,\quad \chi_*=\frac{\chi_1}{\chi_3},\quad \kappa_*=\frac{\kappa_1}{\kappa_3},\quad a_*=\frac{a_3}{a_1}.$$

As the units of length, time, velocity, pressure, and temperature we use $a_1$, $a_1^2/\nu_1$, $\nu_1/a_1$, $\rho_1\nu_1^2/a_1^2$, and $\theta$. The complete nonlinear equations governing Marangoni convection are then written in the dimensionless form

$$\frac{\partial \mathbf{v}_i}{\partial t}+(\mathbf{v}_i\nabla)\mathbf{v}_i=-e_i\nabla p_i+c_i\Delta\mathbf{v}_i, \tag{1}$$

$$\frac{\partial T_i}{\partial t}+\mathbf{v}_i\nabla T_i=\frac{d_i}{P}\Delta T_i, \tag{2}$$

$$\nabla\mathbf{v}_i=0,\quad i=1,2,3, \tag{3}$$

where $e_1=c_1=d_1=1$, $e_2=\rho$, $c_2=1/\nu$, $d_2=1/\chi$, $e_3=\rho_*$, $c_3=1/\nu_*$, $d_3=1/\chi_*$, $\Delta=\nabla^2$, and $P=\nu_1/\chi_1$ is the Prandtl number.

The boundary conditions on the rigid boundaries are

$$\mathbf{v}_1=\mathbf{0},\quad T_1=0\quad \text{at } z=1, \tag{4}$$

$$\mathbf{v}_3=\mathbf{0},\quad T_3=s\quad \text{at } z=-a-a_*, \tag{5}$$

with $s=1$ for heating from below and $s=-1$ for heating from above. The boundary conditions on the deformable interfaces at $z=h$ can be written in the form

$$p_1-p_2+\frac{W_0}{R}(1-\delta_\alpha T_1)+\mathrm{Ga}\,\delta h=\left[\left(\frac{\partial v_{1i}}{\partial x_k}+\frac{\partial v_{1k}}{\partial x_i}\right)-\eta^{-1}\left(\frac{\partial v_{2i}}{\partial x_k}+\frac{\partial v_{2k}}{\partial x_i}\right)\right]n_i n_k, \tag{6}$$

$$\left[\left(\frac{\partial v_{1i}}{\partial x_k}+\frac{\partial v_{1k}}{\partial x_i}\right)-\eta^{-1}\left(\frac{\partial v_{2i}}{\partial x_k}+\frac{\partial v_{2k}}{\partial x_i}\right)\right]\tau_i^{(l)}n_k-\frac{M}{P}\tau_i^{(l)}\frac{\partial T_1}{\partial x_i}=0,\quad l=1,2 \tag{7}$$

$$\mathbf{v}_1=\mathbf{v}_2, \tag{8}$$

$$\frac{\partial h}{\partial t}+v_{1x}\frac{\partial h}{\partial x}+v_{1y}\frac{\partial h}{\partial y}=v_{1z}, \tag{9}$$

$$T_1=T_2, \tag{10}$$

$$\left(\frac{\partial T_1}{\partial x_i}-\kappa^{-1}\frac{\partial T_2}{\partial x_i}\right)n_i=0, \tag{11}$$

and at $z=-a+h_*$,

$$p_2-p_3+\frac{W_{*0}}{R_*}(1-\delta_{\alpha*}T_1)+\mathrm{Ga}\,\delta_* h_*=\left[\eta^{-1}\left(\frac{\partial v_{2i}}{\partial x_k}+\frac{\partial v_{2k}}{\partial x_i}\right)-\eta_*^{-1}\left(\frac{\partial v_{3i}}{\partial x_k}+\frac{\partial v_{3k}}{\partial x_i}\right)\right]n_{*i}n_{*k}, \tag{12}$$

$$\left[\eta^{-1}\left(\frac{\partial v_{2i}}{\partial x_k}+\frac{\partial v_{2k}}{\partial x_i}\right)-\eta_*^{-1}\left(\frac{\partial v_{3i}}{\partial x_k}+\frac{\partial v_{3k}}{\partial x_i}\right)\right]\tau_{*i}^{(l)}n_{*k}-\frac{\overline{\alpha}M}{P}\tau_{*i}^{(l)}\frac{\partial T_3}{\partial x_i}=0,\quad l=1,2 \tag{13}$$

$$\mathbf{v}_2=\mathbf{v}_3, \tag{14}$$

$$\frac{\partial h_*}{\partial t}+v_{3x}\frac{\partial h_*}{\partial x}+v_{3y}\frac{\partial h_*}{\partial y}=v_{3z}, \tag{15}$$

$$T_2=T_3, \tag{16}$$

$$\left(\kappa^{-1}\frac{\partial T_2}{\partial x_i}-\kappa_*^{-1}\frac{\partial T_3}{\partial x_i}\right)n_{*i}=0, \tag{17}$$

where $M=\alpha\theta a_1/\eta_1\chi_1$ is the Marangoni number, $\mathrm{Ga}=ga_1^3/\nu_1^2$ is the Galileo number, $W_0=\sigma_0 a_1/\eta_1\nu_1$, $\delta_\alpha=\alpha\theta/\sigma_0$, $\delta=\rho^{-1}-1$, $W_{*0}=\sigma_{*0}a_1/\eta_1\nu_1$, $\delta_{\alpha_*}=\alpha_*\theta/\sigma_{*0}$, $\delta_*=\rho_*^{-1}-\rho^{-1}$, $\overline{\alpha}=\alpha_*/\alpha$, $R$ and $R_*$ are the radii of curvature, $\mathbf{n}$ and $\mathbf{n}_*$ are the normal vectors, $\boldsymbol{\tau}^{(l)}$ and $\boldsymbol{\tau}_*^{(l)}$ are the tangential vectors of the upper and lower interfaces, and $p_i$ is the difference between the overall pressure and the hydrostatic pressure. The boundary value problem (1)–(17) has the solution

$$\mathbf{v}_i=\mathbf{0},\quad p_i=0\quad (i=1,2,3),\quad h=0,\quad h_*=0, \tag{18}$$

$$T_1=T_1^0=-\frac{s(z-1)}{1+\kappa a+\kappa_* a_*}, \tag{19}$$

$$T_2=T_2^0=-\frac{s(\kappa z-1)}{1+\kappa a+\kappa_* a_*}, \tag{20}$$

$$T_3=T_3^0=-s\frac{\kappa_* z-1+(\kappa_*-\kappa)a}{1+\kappa a+\kappa_* a_*}, \tag{21}$$

corresponding to the mechanical equilibrium state.

Depending on physical parameters of fluids, the mechanical equilibrium state may become unstable with respect to

different instability modes. The short-wavelength instability modes were investigated in the framework of the linear theory in [18–20,24].

The linear theory of the long-wave deformational Marangoni instability was developed in [23]. Because of the existence of two deformable boundaries, one can find in the limit of small wave numbers $k$ two *stationary* instability boundaries $M=M_1$ and $M=M_2$. Also, an *oscillatory* instability boundary may arise, unlike the case of a single interface. In the case where the relative thickness of the bottom layer is small ($a_* \ll 1$), the onset of oscillatory instability was found for two cases

$$\kappa-\kappa_*<0, \quad 1-\eta a^2>0, \quad s>0 \tag{22}$$

(heating from below) and

$$\kappa-\kappa_*>0, \quad 1-\eta a^2<0, \quad s<0 \tag{23}$$

(heating from above). The investigation of nonlinear Marangoni waves generated by the oscillatory instability is the main goal of the present paper.

### III. DERIVATION OF THE AMPLITUDE EQUATIONS

Let us recall the main results of the weakly nonlinear theory for the deformational instability in the case of a sole interface between two fluids (this corresponds to $a_*=0$ in our notation) [13,14]. The deflection of the interface $h$ is equivalent to the local change of the upper and lower layer thicknesses

$$a_1'=1-h, \quad a_2'=a+h. \tag{24}$$

Using expressions (24), it is possible to calculate the critical Marangoni number $M_c$ as a function of $h$. It is necessary to distinguish between the two cases: (a) $Q_1=(dM_c/dh)_{h=0} \neq 0$ and (b) $Q_1=0$. As mentioned in Sec. I, in case (a) we expect that the instability is nonsaturable. In case (b) the instability may be saturable if $Q_2=(d^2M_c/dh^2)_{h=0}>0$.

Indeed, in case (a) the asymptotic analysis [13,14] leads to the amplitude equation (the *Sivashinsky equation* [27])

$$\frac{\partial h^{(0)}}{\partial \tau}=-\Delta_\perp(A\Delta_\perp h^{(0)}+BM^{(1)}h^{(0)}+Ch^{(0)2}), \tag{25}$$

where $h^{(0)}$ is the leading term in the asymptotic expansion of $h=\epsilon h^{(0)}+\cdots$ in powers of a small parameter $\epsilon$, $M^{(1)}=(M-M_c)/\epsilon$, $\tau=\epsilon^2 t$, and $\Delta_\perp$ is the scaled Laplacian operator; the expressions for positive coefficients $A$, $B$, and $C$ are given in Appendix A.

Equation (25) may be written in the form

$$\frac{\partial h^{(0)}}{\partial \tau}=\Delta_\perp \frac{\delta L}{\delta h^{(0)}}, \tag{26}$$

here the Lyapunov functional $L$ is defined as

$$L(h^{(0)})=\int dx\,dy \times\left[\frac{1}{2}A(\nabla_\perp h^{(0)})^2-\frac{1}{2}BM^{(1)}h^{(0)2}-\frac{1}{3}Ch^{(0)3}\right].$$

With the growth of time the functional $L$ decreases. Since it is not bounded from below, the blowup of solutions is possible.

In case (b) one obtains the amplitude equation

$$\frac{\partial h^{(0)}}{\partial \tau}=-\Delta_\perp(A\Delta_\perp h^{(0)}+BM^{(1)}h^{(0)}-Dh^{(0)3}), \tag{27}$$

where $h=\epsilon^{1/2}h^{(0)}+\cdots$; the coefficient $D$, which is defined in Appendix A, is positive if $Q_2>0$. The corresponding Lyapunov functional

$$L(h^{(0)})=\int dx\,dy \times\left[\frac{1}{2}A(\nabla_\perp h^{(0)})^2-\frac{1}{2}BM^{(1)}h^{(0)2}+\frac{1}{4}Dh^{(0)4}\right]$$

is bounded from below. Equation (27), which was derived in the theory of phase transitions, is known as the *Cahn-Hilliard equation* [28]. It describes the formation of two locally stable ''phases'' $h^{(0)}\approx\pm(BM^{(1)}/D)^{1/2}$ separated by kinks [29].

In the case of a system with two interfaces one obtains two stationary instability boundaries $M=M_1$ and $M=M_2$ and in certain cases [see Eqs. (22) and (23)] also the oscillatory instability boundary $M=M_0$. If $M_1$ and $M_2$ are not close to each other, the deformations of both interfaces $h$ and $h_*$ near each instability threshold are mutually proportional and the problem is governed by Eq. (25) or (27). If $M_1$ and $M_2$ are close and in the case of the oscillatory instability, the deformations of both interfaces can be considered as independent active variables and we can expect that the problem is governed by a system of *two coupled equations* of the type (25) or (27).

We are going to derive the system of amplitude equations for an oscillatory instability in a specific case of a very thin bottom layer $a_* \ll 1$. According to [23], the threshold Marangoni number of the oscillatory instability is

$$M=M_0=\frac{2s\,\mathrm{Ga}\delta Pa(1+\eta a)(1+\kappa a)^2}{3\kappa(1+a)(1-\eta a^2)}+o(1) \tag{28}$$

and the frequency of oscillations in the long-wave limit $k\to 0$ is determined by formulas

$$\omega=\omega^{(2)}k^2+\cdots,$$
$$\omega^{(2)}=\mathrm{Ga}\delta a^2\left[\frac{(1+\eta a)\,\eta\eta_*(\kappa_*-\kappa)}{18J\kappa(1+a)(1-\eta a^2)}\right]^{1/2}a_*+o(a_*), \tag{29}$$

where

$$J=\eta^2a^4+4\eta a^3+6\eta a^2+4\eta a+1.$$

The deflection of the interface (24) leads to the following change of the critical Marangoni number (see Appendix B):

$$M_0=\frac{2s\,\mathrm{Ga}\delta P(1-h)(a+h)[(1-h)+\eta(a+h)][(1-h)+\kappa(a+h)]^2}{3\kappa(1+a)[(1-h)^2-\eta(a+h)^2]}+o(1),\quad -a<h<1. \tag{30}$$

The expressions for $Q_1=(dM_0/dh)_{h=0}$ and $Q_2=(d^2M_0/dh^2)_{h=0}$, which are important for the nonlinear analysis, are given in the Appendix B. Cases (a) $Q_1\neq 0$ and (b) $Q_1=0,\ Q_2>0$ are considered separately.

### A. The case $Q_1\neq 0$

Let us consider the region near the threshold of oscillatory instability

$$M=M_0+ma_*,\quad m=O(1). \tag{31}$$

The linear theory predicts an oscillatory instability in the region of small wave numbers $k=O(a_*^{1/2})$. This instability is characterized by both the growth rate and the frequency of oscillations of $O(a_*^2)$. From expression (30) we can expect that the deformations $h=O(a_*)$ are relevant in the case $Q_1\neq 0$. Taking into account the scaling properties of eigenfunctions appearing in the linear theory, we introduce the scaling of variables

$$\begin{gathered}\overline{x}=a_*^{1/2}x,\quad \overline{y}=a_*^{1/2}y,\quad \overline{t}=a_*^2t,\quad h=a_*\overline{h},\\ T_j=T_j^0+a_*\Theta_j,\quad p_j=a_*P_j,\quad \mathbf{v}_{j\perp}=a_*^{3/2}\mathbf{V}_{j\perp},\\ v_{jz}=a_*^2V_{jz}\quad (j=1,2),\\ h_*=a_*^2\overline{h}_*,\quad T_3=s+a_*\Theta_3,\quad p_3=a_*P_3,\\ \mathbf{v}_{3\perp}=a_*^{5/2}\mathbf{V}_{3\perp},\quad v_{3z}=a_*^4V_{3z},\end{gathered} \tag{32}$$

where $\mathbf{v}_{m\perp}\equiv(v_{mx},v_{my})$, $m=1,2,3$. In the region $-a-a_*\leqslant z\leqslant -a$ the variable

$$\overline{z}=(z+a)/a_* \tag{33}$$

is used.

The solution $f=(H,H_*,\Theta_m,P_m,\mathbf{V}_{m\perp},V_{mz})$ $(m=1,2,3)$ is presented in the form of a series

$$f=f^{(0)}+a_*f^{(1)}+\cdots. \tag{34}$$

We substitute the expansions (31)–(34) into the problem (1)–(17) and collect the terms of the same order in $a_*$. We obtain the amplitude equations for ''active'' variables $H$ and $H_*$ from the solvability conditions. The details of the derivation of the amplitude equations are relegated to Appendix C. Here we describe the main steps of the derivation.

In zeroth order, the equations and boundary conditions are linear. We reproduce the results of the linear theory in the long-wavelength limit [23], including the expression (28) for the critical Marangoni number of the oscillatory instability, and obtain the equation

$$\frac{\partial\overline{h}_*^{(0)}}{\partial\overline{t}}=E\overline{\Delta}_\perp\overline{h}^{(0)}, \tag{35}$$

where

$$E=\frac{\mathrm{Ga}\delta}{6}\frac{\eta_*a}{1-\eta a^2},\quad \overline{\Delta}_\perp=\frac{\partial^2}{\partial\overline{x}^2}+\frac{\partial^2}{\partial\overline{y}^2},$$

which describes in the leading order the time evolution of the deformation of the lower interface.

In the first order in $a_*$ we obtain the nonlinear amplitude equation for the evolution of the deformation of the upper interface

$$\frac{\partial\overline{h}^{(0)}}{\partial\overline{t}}=-\overline{\Delta}_\perp[A\overline{\Delta}_\perp\overline{h}^{(0)}+B(m-m_*)\overline{h}^{(0)}+C\overline{h}^{(0)2}+F\overline{h}_*^{(0)}], \tag{36}$$

where the coefficients $A,B,C$ are *exactly* the same as in Eq. (25), the quantity $m_*$ describing the deviation of the critical Marangoni number from the value $M_0$ in the first order in $a_*$ is calculated in Appendix C, and

$$F=\frac{sM_0(\kappa_*-\kappa)\eta a^2(1-\eta a^2)}{2P(1+\kappa a)^2J}.$$

Thus we obtained the *coupled* system of amplitude equations (35) and (36) describing the nonlinear evolution of long-wavelength deformations of both interfaces near the instability threshold in the case $a_*\ll 1$. Let us note that Eqs. (35) and (36) predict a linear oscillatory instability with the frequency $\omega=\sqrt{EF}k^2+O(k^4)$ in the case of $E$ and $F$ having the same sign, which coincides with formula (29).

### B. The case $Q_1=0$

In the case $Q_1=0$, the nonlinear coefficient $C$ in Eq. (36) vanishes. In order to obtain the nonlinear saturation, it is necessary to use a different scaling of functions

$$\begin{gathered}h=a_*^{1/2}\overline{h},\quad T_j=T_j^0+a_*^{1/2}\Theta_j,\quad p_j=a_*^{1/2}P_j,\\ \mathbf{v}_{j\perp}=a_*\mathbf{V}_{j\perp},\quad v_{jz}=a_*^{3/2}V_{jz}\quad (j=1,2),\\ h_*=a_*^{3/2}\overline{h}_*,\quad T_3=s+a_*^{1/2}\Theta_3,\quad p_3=a_*^{1/2}P_3,\\ \mathbf{v}_{3\perp}=a_*^2\mathbf{V}_{3\perp},\quad v_{3z}=a_*^{7/2}V_{3z}.\end{gathered} \tag{37}$$

The solution is expanded into series in powers of $a_*^{1/2}$. Finally, Eq. (35) is not changed, while Eq. (36) is replaced by the amplitude equation

$$\frac{\partial \overline{h}^{(0)}}{\partial \overline{t}} = -\overline{\Delta}_\perp [A\overline{\Delta}_\perp \overline{h}^{(0)} + B(m-m_*)\overline{h}^{(0)} - D\overline{h}^{(0)3} + F\overline{h}_*^{(0)}], \tag{38}$$

where the coefficient $D$ is the same as in Eq. (27).

In the case of small but nonzero $Q_1$, where the coefficient $C$ is not exactly equal to zero but small, $C=\overline{C}a_*^{1/2}$, $\overline{C}=O(1)$, the equation containing both quadratic and cubic nonlinearities is obtained (see [13]):

$$\frac{\partial \overline{h}^{(0)}}{\partial \overline{t}} = -\overline{\Delta}_\perp [A\overline{\Delta}_\perp \overline{h}^{(0)} + B(m-m_*)\overline{h}^{(0)} + \overline{C}\overline{h}^{(0)2} - D\overline{h}^{(0)3} + F\overline{h}_*^{(0)}]. \tag{39}$$

Equations (36) and (38) can be considered as particular cases of Eq. (39). By means of the transformation

$$\overline{h}=(FE/D^2)^{1/4}H, \quad \overline{h}_*=(E^3/FD^2)^{1/4}H_*,$$
$$X=(FE/A^2)^{1/4}\overline{x}, \quad Y=(FE/A^2)^{1/4}\overline{y}, \quad \tau=(FE/A)\overline{t}, \tag{40}$$

Eqs. (39) and (35) are rewritten in the form

$$\frac{\partial H}{\partial \tau} + \Delta_\perp(\Delta_\perp H + \mu H + \gamma H^2 - H^3 + H_*) = 0, \tag{41}$$

$$\frac{\partial H_*}{\partial \tau} - \Delta_\perp H = 0, \tag{42}$$

where

$$\Delta_\perp = \frac{\partial}{\partial X^2} + \frac{\partial}{\partial Y^2}, \quad \mu = \frac{B(m-m_*)}{(FE)^{1/2}}, \quad \gamma = \frac{\overline{C}}{(FED^2)^{1/4}}.$$

## IV. TRAVELING WAVE SOLUTIONS

The trivial solution $H=0$, $H_*=0$ of the system (41) and (42) is stable with respect to disturbances with the wave number $k$ in the region $\mu<k^2$. On the neutral curve $\mu=\mu_0=k^2$, an oscillatory instability with the frequency $\omega_0=\pm k^2$ appears. In the present section, we consider small-amplitude solutions that bifurcate on the neutral curve.

### A. Bifurcation of traveling wave solutions

In order to describe the traveling wave solutions near the neutral curve [$\mu-\mu_0=O(\epsilon^2)$, $\epsilon \ll 1$], we introduce the time scales

$$\tau_0=\tau, \quad \tau_2=\epsilon^2\tau, \ldots \tag{43}$$

and use the expansions

$$\mu=\mu_0+\epsilon^2\mu_2, \quad H=\epsilon H_1+\epsilon^2 H_2+\cdots,$$
$$H_*=\epsilon H_{*1}+\epsilon^2 H_{*2}+\cdots. \tag{44}$$

In the first order in $\epsilon$, we obtain a linear eigenvalue problem. Let us consider a particular solution corresponding to a traveling wave that propagates along the $X$ axis in the positive direction and has the wave number $k$. We choose

$$H_1=A(\tau_2)e^{i(kX-\omega_0\tau_0)}+\text{c.c.},$$
$$H_{*1}=B(\tau_2)e^{i(kX-\omega_0\tau_0)}+\text{c.c.}$$

(c.c. means complex conjugate) and find $\mu_0=k^2$, $\omega_0=k^2$, and $B=-iA$. In the second order, the solution is

$$H_2=A_2(\tau_2)e^{2i(kX-\omega_0\tau_0)}+\text{c.c.},$$
$$H_{*2}=B_2(\tau_2)e^{2i(kX-\omega_0\tau_0)}+\text{c.c.}$$

(we omit the general solution of the homogeneous system by renormalizing the amplitude), where

$$A_2=\frac{2\gamma A^2}{3(i+2k^2)}, \quad B_2=-2iA_2.$$

The solvability condition for the third-order equations determines the Landau equation for the amplitude evolution:

$$\frac{dA}{d\tau_2}=\frac{k^2}{2}\left\{\mu_2 A+\left[\frac{4\gamma^2(2k^2-i)}{3(1+4k^4)}-3\right]|A|^2A\right\}. \tag{45}$$

The limit cycle corresponding to a traveling wave solution is $A=|A|\exp(i\omega_2\tau_2)$, where

$$\omega_2=\frac{2\gamma^2k^2}{3(1+4k^4)}, \tag{46}$$

$$|A|^2=\mu_2\left[3-\frac{8\gamma^2k^2}{3(1+4k^4)}\right]^{-1}. \tag{47}$$

One can see that the bifurcation is supercritical for any values of $k$ if $\gamma<3/\sqrt{2}$. Otherwise, an interval of a subcritical bifurcation appears in a certain interval of $k$.

### B. Interaction of traveling waves

In order to consider the interaction of traveling waves, we use the same scales (43) and expansions (44) as in the preceding subsection, but in the leading order of the expansion we choose the solution

$$H_1=A^{(1)}(\tau_2)e^{i(\mathbf{k}^{(1)}\cdot\mathbf{X}-\omega_0\tau_0)}+A^{(2)}(\tau_2)e^{i(\mathbf{k}^{(2)}\cdot\mathbf{X}-\omega_0\tau_0)}\text{c.c.},$$

$$H_{*1}=B^{(1)}(\tau_2)e^{i(\mathbf{k}^{(2)}\cdot\mathbf{X}-\omega_0\tau_0)}+B^{(2)}(\tau_2)e^{i(\mathbf{k}^{(2)}\cdot\mathbf{X}-\omega_0\tau_0)}\text{c.c.},$$

$|\mathbf{k}^{(1)}|=|\mathbf{k}^{(2)}|=k$, $\omega_0=k^2$, $B^{(1)}=-iA^{(1)}$, and $B^{(2)}=-iA^{(2)}$, corresponding to two traveling waves moving in different directions. In the second order, the solution has the structure

$$H_2=A_2^{(1,1)}(\tau_2)e^{2i(\mathbf{k}^{(1)}\cdot\mathbf{X}-\omega_0\tau_0)}+A_2^{(2,2)}(\tau_2)e^{2i(\mathbf{k}^{(2)}\cdot\mathbf{X}-\omega_0\tau_0)}$$
$$+A_2^{(1,2)}(\tau_2)e^{2i(\mathbf{k}^{(1)}+\mathbf{k}^{(2)})\cdot\mathbf{X}-2\omega_0\tau_0)}$$
$$+A_2^{(1,-2)}(\tau_2)e^{2i(\mathbf{k}^{(1)}-\mathbf{k}^{(2)})\cdot\mathbf{X}}+\text{c.c.},$$

$$H_{*2}=B_2^{(1,1)}(\tau_2)e^{2i(\mathbf{k}^{(1)}\cdot\mathbf{X}-\omega_0\tau_0)}+B_2^{(2,2)}(\tau_2)e^{2i(\mathbf{k}^{(2)}\cdot\mathbf{X}-\omega_0\tau_0)}$$
$$+B_2^{(1,2)}(\tau_2)e^{2i(\mathbf{k}^{(1)}+\mathbf{k}^{(2)})\cdot\mathbf{X}-2\omega_0\tau_0)}$$
$$+B_2^{(1,-2)}(\tau_2)e^{2i(\mathbf{k}^{(1)}-\mathbf{k}^{(2)})\cdot\mathbf{X}}+\text{c.c.}$$

(as before, we omit the general solution of the homogeneous system). We obtain the following expressions for the coefficients:

$$A_2^{(1,1)}=\frac{2\gamma A^{(1)2}}{3(i+2k^2)},\quad B_2^{(1,1)}=-2iA_2^{(1,1)},$$

$$A_2^{(2,2)}=\frac{2\gamma A^{(2)2}}{3(i+2k^2)},\quad B_2^{(2,2)}=-2iA_2^{(2,2)},$$

$$A_2^{(1,2)}=\frac{2\gamma(1+\zeta)A^{(1)}A^{(2)}}{i\zeta(2+\zeta)+(1+\zeta)(1+2\zeta)k^2},$$

$$B_2^{(1,2)}=-i(1+\zeta)A_2^{(1,2)},$$

$$A_2^{(1,-2)}=0,\quad B^{(1,-2)}=-\gamma A^{(1)}A^{(2)*},$$

where $\zeta=\mathbf{k}^{(1)}\cdot\mathbf{k}^{(2)}/k^2$. The solvability condition for the third-order equations determines a pair of Landau equations for the amplitudes evolution:

$$\frac{dA^{(1)}}{d\tau_2}=\frac{k^2}{2}[\mu_2A^{(1)}-\lambda_0|A^{(1)}|^2A^{(1)}-\lambda(\zeta)|A^{(2)}|^2A^{(1)}],$$

$$\frac{dA^{(2)}}{d\tau_2}=\frac{k^2}{2}[\mu_2A^{(2)}-\lambda_0|A^{(2)}|^2A^{(2)}-\lambda(\zeta)|A^{(1)}|^2A^{(2)}],\tag{48}$$

where

$$\lambda_0=3-\frac{4\gamma^2(2k^2-i)}{3(1+4k^2)},\tag{49}$$

$$\lambda(\zeta)=6-\frac{4\gamma^2(1+\zeta)[(k^2(1+\zeta)(1+2\zeta)-i\zeta)(2+\zeta)]}{k^4(1+\zeta)^2(1+2\zeta)^2+\zeta^2(2+\zeta)^2}.\tag{50}$$

The system of equations (48) describes the nonlinear evolution of two interacting harmonic waves. It can be easily shown that in the case where $0<\mathrm{Re}\,\lambda_0<\mathrm{Re}\,\lambda(\zeta)$ for any $\zeta$ (Re denotes the real part), the one-dimensional traveling wave solutions $|A^{(1)}|^2=\mu_2/\mathrm{Re}\,\lambda_0$, $|A^{(2)}|^2=0$ and $|A^{(2)}|^2=\mu_2/\mathrm{Re}\,\lambda_0$, $|A^{(1)}|^2=0$ are stable as $\mu_2>0$ in frames of the system (48). In the case $\mathrm{Re}\,\lambda(\zeta)<\mathrm{Re}\,\lambda_0$, the nonlinear superposition of two waves $|A^{(1)}|^2=|A^{(2)}|^2=\mu_2/[\mathrm{Re}\,\lambda_0+\mathrm{Re}\,\lambda(\zeta)]$ is stable if $\mu_2>0$, $\mathrm{Re}\,\lambda_0+\mathrm{Re}\,\lambda(\zeta)>0$.

Using expressions (49) and (50), we find that the necessary condition of the stability of one-dimensional traveling wave solutions is

$$\mathrm{Re}[\lambda(\zeta)-\lambda_0]=3+k^2\gamma^2\left[\frac{8}{3(4k^4+1)}-\frac{4(1+\zeta)^2(1+2\zeta)}{k^4(1+\zeta)^2(1+2\zeta)^2+\zeta^2(2+\zeta)^2}\right]>0.\tag{51}$$

If $\gamma=0$ [the quadratic term in the Eq. (41) is absent] the one-dimensional traveling wave is stable with respect to disturbances with the same wave number moving in any direction.

If $\gamma$ is small, the expression (51) is negative only in the region of small wave numbers, $|k|<\sqrt{4/3}\gamma+O(\gamma^5)$, and positive otherwise. The expression (51) is minimal for small values of the parameter $\zeta$: $\zeta\approx-k^4/4$. Thus the transition to nearly square patterns is expected for sufficiently small $k$. Let us note that square patterns were predicted in the case of the dispersion relation $\omega\sim k^2$ by Pismen [30]. For finite values of $\gamma$, the traveling wave is unstable with respect to disturbances with $\zeta=0$, generating square patterns, if its wave number satisfies the relation $|k|<k_*(\gamma)$, where

$$\gamma^2=\frac{9k^2(4k^4+1)}{4(3+10k^4)}.$$

### C. Finite-amplitude traveling waves

In the previous subsections, we analyzed small-amplitude traveling waves near the neutral curve. Now we shall consider finite-amplitude spatially periodic traveling wave solutions

$$H=H(\xi),\quad H_*=H_*(\xi),\quad \xi=X-c\tau,\tag{52}$$

$$H(\xi+L)=H(\xi),\quad H_*(\xi+L)=H_*(\xi).\tag{53}$$

Substituting Eq. (52) into Eqs. (41) and (42), eliminating $H_*(\xi)$, and integrating once the obtained equation, we arrive at

$$H_{\xi\xi\xi}-\frac{H_{\xi\xi}}{c}+\mu H_\xi-cH+(\gamma H^2-H^3)_\xi=-c\langle H\rangle,\tag{54}$$

where the subscript $\xi$ denotes differentiation with respect to $\xi$ and the integration constant

$$\langle H\rangle=\frac{1}{L}\int_0^L H(\xi)d\xi$$

is the mean value of the function $H(\xi)$ and therefore should be set equal to zero because $H(\xi)$ is proportional to the deviation of the fluid level from its mean value.

Spatially periodic waves (52) and (53) correspond to limit cycles of the dynamical system (54). Equation (54) with the periodicity condition $H(\xi+L)=H(\xi)$ is a nonlinear eigenvalue problem for the phase velocity $c(L)$. Because the dependence $c(L)$ is *a priori* unknown, we actually treated in our calculations the velocity $c$ as a free parameter and computed the corresponding value of the limit cycle's period $L(c)$.

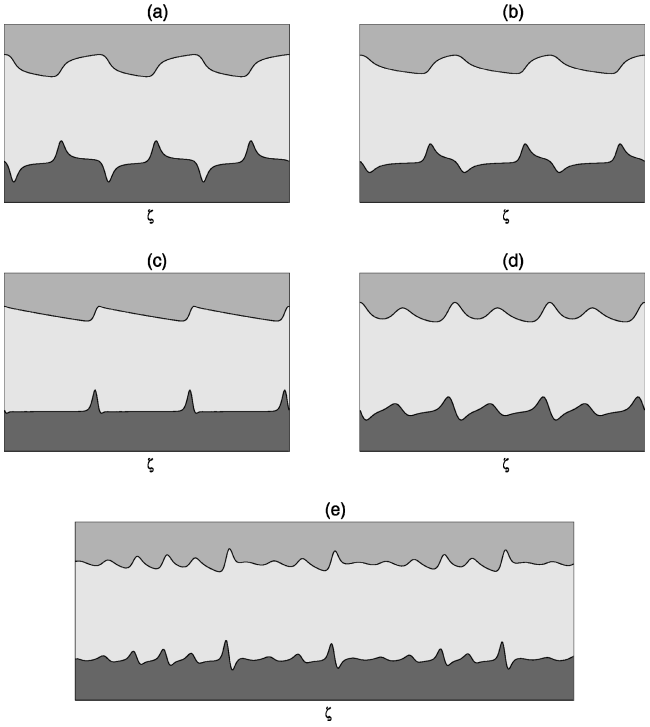


FIG. 2. Examples of traveling wavetrains according to Eq. (56): (a) $\gamma=0$, $c=-0.222$, $\mu=2$; (b) $\gamma=1$, $c=-0.08$, $\mu=0.368$; (c) $\gamma=5$, $c=-0.36033$, $\mu=0.03$; (d) $\gamma=3$, $c=-1$, $\mu=0.7$; (e) $\gamma=3$, $c=-0.8$, $\mu=0.368$.

Equation (54) can be simplified in the limiting case of small $c$. Multiplying Eq. (54) by $H$ and integrating over the period, we find that $\langle H_\xi^2\rangle = c^2\langle H^2\rangle$. Thus the limit $c\to 0$ corresponds to the long-wavelength limit $L\to\infty$.

In this long-wavelength limit, it is convenient to use the variable $\zeta = c\xi$ and to rewrite Eq. (54) in the form

$$-c^2 H_{\zeta\zeta\zeta} + H_{\zeta\zeta} + (H^3 - \gamma H^2 - \mu H)_\zeta + H = 0. \tag{55}$$

Let us note that $H_* = -H_\zeta$. In the limit $c\to 0$, if the periodic solutions of Eq. (55) reveal no boundary layers, they tend to the periodic solutions of the second-order equation

$$H_{\zeta\zeta} + (H^3 - \gamma H^2 - \mu H)_\zeta + H = 0. \tag{56}$$

For the case $\gamma=0$ where the traveling waves are expected to be stable with respect to two-dimensional disturbances, Eq. (56) turns into the familiar case of the Van der Pol equation [31]. The latter is known to yield limit cycles whose shape varies from harmonic oscillations (in the case of small $\mu$) to the strongly nonlinear relaxation oscillations for large values of $\mu$. In the case of nonzero $\gamma$ the invariance of the equation with respect to the change of sign of $H$ is broken: The relaxationlike oscillations are still observed, but the characteristic Van der Pol symmetry between the humps and the troughs is absent.

Some additional simplification of Eq. (56) can be obtained in the limit $\gamma \gg 1$, $\mu \ll 1$. If we assume that $H = \gamma^{-1}\tilde{H}$ and $\tilde{H} = O(1)$ and omit the term containing $\mu$, we find in the leading order

$$\tilde{H}_{\zeta\zeta} - (\tilde{H}^2)_\zeta + \tilde{H} = 0. \tag{57}$$

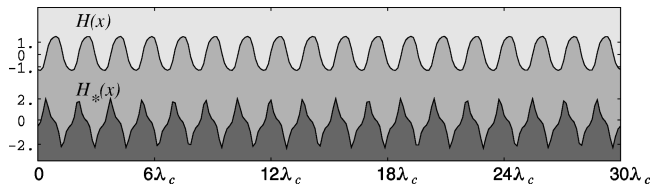


FIG. 3. Traveling wave for $\mu=2$ and $\gamma=0$. The initial condition is a small-amplitude random field.

The trajectory corresponding to the unbounded solution

$$\tilde{H} = \zeta/2 \tag{58}$$

separates the phase plane $(\tilde{H}, \tilde{H}_* = -\tilde{H}_\zeta)$ into two regions. In the region $\tilde{H}_* < -1/2$ the trajectories tend to infinity as $\zeta \to \pm\infty$. The half plane $\tilde{H}_* > -1/2$ is filled by periodic orbits determined by the equation

$$\tilde{H}_* - \ln(1+2\tilde{H}_*) + \frac{1}{2}\tilde{H}^2 = E, \quad E = \text{const} > 0.$$

If $E \gg 1$, the wave relief has a ''sawlike'' shape. On a long interval of the length $O(\sqrt{E})$, $\tilde{H}_* = -1/2 + O(\exp(-E))$, so that the relief of $\tilde{H}$ is exponentially close to the linear profile (58). On a short interval of the length $O(1/\sqrt{E})$, $\tilde{H}_* > 0$, and $\tilde{H}_* = O(E)$, which corresponds to a steep wave front of $\tilde{H}$.

The typical wave profiles $H(\zeta)$ and $H_*(\zeta)$ calculated by means of the symmetric ($\gamma=0$) and ''asymmetric'' ($\gamma=1$) equation (55) are plotted in Figs. 2(a) and 2(b), respectively. These two plots, as well as Figs. 2(c) and 2(d), present the longitudinal shape of the waves in the correct way. On the contrary, the vertical displacements, as related to the thicknesses of the layers, cannot be recovered from the equations and therefore are represented only qualitatively.

In the case of vanishing or small values of $\gamma$ this regular pattern with one hump on a period is the only nontrivial bounded solution of Eq. (54) and exists only for positive values of $\mu$; the velocity of the traveling waves obeys the inequality $c^2 < \mu$ and for each value of $c$ there exists only one periodic solution. The situation changes for $\gamma > \sqrt{3}$ when the above inequality does not necessarily hold. In this case the increase of $\mu$ can create the finite-amplitude periodic solutions through a saddle-node bifurcation. Under $\gamma > 2.8$ the traveling waves of this kind can be found even for negative values of $\mu$. For sufficiently large $\gamma$, the upper interface displays the characteristic sawlike oscillations, whereas the lower one is built of the long, almost horizontal segments separated by short elevations [Fig. 2(c)].

Moderate and large values of $\gamma$ allow for more complicated patterns of traveling waves: In this parameter domain one encounters further bifurcations of periodic solutions, which include cascades of period doublings (in fact, these doublings with respect to the variable $\xi$ are doublings of the spatial period) and the onset of chaotic wave profiles. Respective deformations of the interfaces are plotted in Figs. 2(d) and 2(e). In the last three cases the periodic pattern delivered by Eq. (55) under the fixed values of $\gamma$ and $\mu$ for a given velocity $c$ is not unique (in the very last case there is apparently an infinity of different periodic solutions).

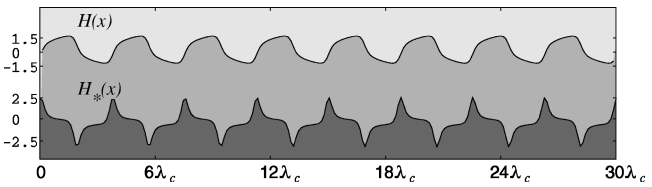


FIG. 4. Traveling wave for $\mu=2$ and $\gamma=0$. The initial condition is a regular function of $O(1)$.

## V. NUMERICAL SIMULATION OF THE AMPLITUDE EQUATIONS

The one-dimensional version of Eqs. (41) and (42)

$$\frac{\partial H}{\partial \tau}+\frac{\partial^2}{\partial X^2}\left(\frac{\partial^2 H}{\partial X^2}+\mu H+\gamma H^2-H^3+H_*\right)=0, \quad (59)$$

$$\frac{\partial H_*}{\partial \tau}-\frac{\partial^2 H}{\partial X^2}=0 \quad (60)$$

was simulated numerically under periodic boundary conditions. The pseudospectral technique was employed for the spatial discretization and the Adams scheme for the time advance. The standard routines CO6EAF and CO6EBF for the fast Fourier transform and DO2CBF for the Adams scheme from the NAG routines library were used. The number of spatial discretization points was chosen in such a way that the typical wavelength $\lambda_c=2\pi/k_c$ of the most unstable (in linear approximation) mode with wave number $k_c$ was covered by at least ten points. The latter ensures fair resolution of the calculated solution. The time step was chosen automatically.

Both small-amplitude random fields and regular functions with amplitudes of $O(1)$ were used as initial data in all simulations. In a number of cases the result of evolution depends on initial conditions. This means that Eqs. (59) and (60) have different coexisting attractors. We considered the same values of parameters ($\gamma$, $\mu$) as in Fig. 2.

For the parameters values of $\gamma$ and $\mu$ from Fig. 2(a) two different interfacial configurations were obtained: Random small-amplitude initial conditions evolved to the profile shown in Fig. 3, whereas the regular $O(1)$ initial conditions settled to the wave plotted in Fig. 4. Interfaces form the traveling waves moving with velocities $c=-0.0015$ and $c=-0.01$, respectively. In both cases the typical wave scale is larger than that predicted by the linear theory, $\lambda_c$.

A few different interfacial configurations were observed for the pair $\mu=0.368$, $\gamma=1$ [Fig. 2(b)]. Depending on the initial conditions, the number of the humps for the settled wave states within the domain varies between 1 and 6; compared to the results of the linear stability analysis, the wavelength is noticeably larger. Figure 5 shows the interfaces with four typical humps that form the traveling wave moving with the velocity $c=-0.001\,97$. Only the blowup for all tested initial conditions was observed in final stage of evolution for the pair $\mu=0.03$, $\gamma=1$.

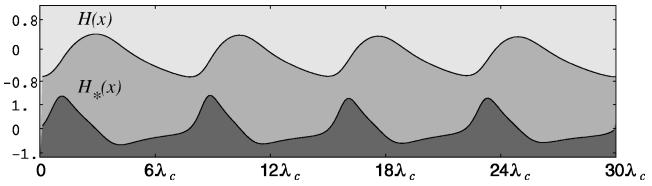


FIG. 5. Traveling wave for $\mu=0.368$ and $\gamma=1$.

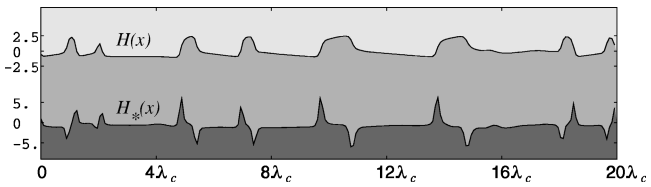


FIG. 6. Typical interfacial profiles for $\mu=0.7$ and $\gamma=3$.

Typical irregular interfacial profiles observed for the pairs $\mu=0.7$, $\gamma=3$ [Fig. 2(d)] and $\mu=0.368$, $\gamma=3$ [Fig. 2(e)] are shown in Figs. 6 and 7, respectively. The dynamics, observed for all initial conditions, are unsteady. The typical wave scale in both cases is larger than $\lambda_c$. The question of stability of one-dimensional regimes in the framework of the partial differential equations (41) and (42) as well as their evolution with respect to the two-dimensional perturbations must be studied separately and lies outside the range of our current research.

## VI. CONCLUSIONS

We have shown that the weakly nonlinear regimes of the long-wave Marangoni instability in a system with two interfaces in the case where one of the fluid layers is thin are governed by the Cahn-Hilliard equation coupled with a certain linear equation. In the absence of the quadratic nonlinear term, the periodic traveling waves are generated rather than kinks that are typical for the pure Cahn-Hilliard equation. Numerical simulation reveals multistability of wavy regimes. If the quadratic nonlinear interaction is present, one can expect the onset of two-dimensional wavy patterns. Investigation of such patterns remains beyond the scope of the present paper.

## ACKNOWLEDGMENTS

This work was supported in part by the German-Israeli Foundation for Scientific Research and Development under Research Contract No. I 0460-228.10/95. I.B.S. acknowledges the support of the Israeli Ministry of Science and Humanities and the Israeli Ministry for Immigrant Absorption.

## APPENDIX A

The equations (25) and (27) describing the evolution of an interface in the case of a stationary long-wavelength instability were derived in [14] (see also [13]). Here we present the expressions for the coefficients appearing in these equations:

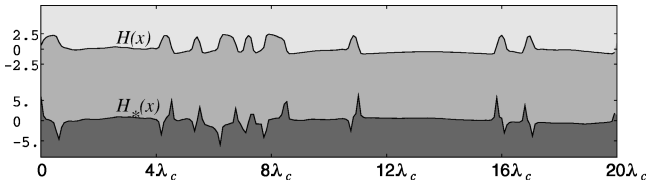


FIG. 7. Typical interfacial profiles for $\mu=0.368$ and $\gamma=3$.

$$A=\zeta N,\quad B=\frac{\zeta}{M_c},\quad C=-\frac{\zeta K_1}{2},\quad D=-\frac{\zeta K_2}{6}, \tag{A1}$$

where

$$\zeta=\frac{\mathrm{Ga}\delta\eta a^3(1+\eta a)}{3S},$$

$$S=1+4\eta a+6\eta a^2+4\eta a^3+\eta^2 a^4; \tag{A2}$$

$$N=\frac{(\kappa-1)a(1-a)}{3(1+\kappa a)}+\frac{(\eta+a)a}{15(1+\eta a)}+\frac{2(1-\eta)a^2}{15(1-\eta a^2)}+\frac{W}{\mathrm{Ga}\delta}+\frac{P(1-\chi a^2)\eta a^3\mathrm{Ga}\delta}{120(1+a)(1-\eta a^2)}; \tag{A3}$$

$$M_c=\frac{2sP\,\mathrm{Ga}\delta(1+\kappa a)^2 a(1+\eta a)}{\kappa(1+a)(1-\eta a^2)}; \tag{A4}$$

$$K_1=\frac{\eta(1+a)}{1+\eta a}+\frac{2\kappa(1+a)}{1+\kappa a}+\frac{1-2a}{a}+\frac{2\eta a(1+a)}{1-\eta a^2}; \tag{A5}$$

$$K_2=-\frac{\eta-1}{1+\eta a}-\frac{\kappa-1}{1+\kappa a}-\frac{1}{a}-\frac{1+2\eta a}{1-\eta a^2}+\frac{(\eta-1)(\kappa-1)}{(1+\eta a)(1+\kappa a)}+\frac{\eta-1}{a(1+\eta a)}+\frac{(\eta-1)(1+2\eta a)}{(1-\eta a^2)(1+\eta a)}+\frac{\kappa-1}{a(1+\kappa a)}+\frac{(\kappa-1)(1+2\eta a)}{(1+\kappa a)(1-\eta a^2)}+\frac{1+2\eta a}{a(1-\eta a^2)}+\frac{\eta}{1-\eta a^2}+\left(\frac{1+2\eta a}{1-\eta a^2}\right)^2. \tag{A6}$$

## APPENDIX B

A uniform deflection of the upper interface (24) is equivalent to the local change of the upper and middle layer thicknesses (in dimensional variables)

$$a_1'=a_1(1-h),\quad a_2'=a_2+ha_1.$$

The onset of convection instability is determined by the parameters

$$M'=\frac{\alpha\theta a_1'}{\eta_1\chi_1},\quad \mathrm{Ga}'=\frac{g a_1'^3}{\nu_1^2},\quad a'=\frac{a_2'}{a_1'}.$$

According to Eq. (28), the threshold is governed by the formula

$$M_0'=\frac{2s\,\mathrm{Ga}'\delta P(1+\eta a')(1+\kappa a')^2}{3\kappa(1+a')(1-\eta a'^2)}+o(1).$$

Returning to variables $M$, Ga, and $\delta$, we rewrite the latter equation in the form (30). The parameter $h$ can vary within the interval $-a<h<1$. The expressions for variables $Q_1=(dM_0/dh)_{h=0}$ and $Q_2=(d^2M_0/dh^2)_{h=0}$ are directly connected with those of $K_1$ and $K_2$ [see Eqs. (A5) and (A6)]:

$$Q_1=K_1M_0,\quad Q_2=K_2M_0.$$

## APPENDIX C

In the present appendix we describe some details of the derivation of the amplitude equations (35) and (36). Substituting the expressions (31)–(34) into the problem (1)–(17), we obtain the following system of equations and boundary conditions:

$$-\bar{\nabla}_\perp P_1+\frac{\partial^2\mathbf{V}_{1\perp}}{\partial z^2}+a_*-\bar{\Delta}_\perp\mathbf{V}_{1\perp}=O(a_*^2), \tag{C1}$$

$$-\frac{\partial P_1}{\partial z}+a_*\frac{\partial^2 V_{1z}}{\partial z^2}=O(a_*^2), \tag{C2}$$

$$a_*V_{1z}A_1^0+O(a_*^2)=\frac{1}{P}\frac{\partial^2\Theta_1}{\partial z^2}+\frac{a_*}{P}\bar{\Delta}_\perp T_1, \tag{C3}$$

$$\frac{\partial V_{1z}}{\partial z}+\bar{\nabla}_\perp\cdot\mathbf{V}_{1\perp}=0, \tag{C4}$$

$$-\rho\bar{\nabla}_\perp P_2+\frac{1}{\nu}\frac{\partial^2\mathbf{V}_{2\perp}}{\partial z^2}+\frac{a_*}{\nu}\bar{\Delta}_\perp\mathbf{V}_{2\perp}=O(a_*^2), \tag{C5}$$

$$-\rho\frac{\partial P_2}{\partial z}+\frac{a_*}{\nu}\frac{\partial^2 V_{2z}}{\partial z^2}=O(a_*^2), \tag{C6}$$

$$a_*V_{2z}A_2^0+O(a_*^2)=\frac{1}{\chi P}\frac{\partial^2\Theta_2}{\partial z^2}+\frac{a_*}{\chi P}\bar{\Delta}_\perp T_2, \tag{C7}$$

$$\frac{\partial V_{2z}}{\partial z}+\bar{\nabla}_\perp\cdot\mathbf{V}_{2\perp}=0, \tag{C8}$$

$$-\rho_*a_*\bar{\nabla}_\perp P_3+\frac{1}{\nu_*}\frac{\partial^2\mathbf{V}_{3\perp}}{\partial\bar{z}^2}=O(a_*^3), \tag{C9}$$

$$-\rho_*\frac{\partial P_3}{\partial\bar{z}}=O(a_*^2), \tag{C10}$$

$$\frac{1}{\chi_*P}\frac{\partial^2\Theta_3}{\partial\bar{z}^2}=O(a_*^2), \tag{C11}$$

$$\frac{\partial V_{3z}}{\partial\bar{z}}+\bar{\nabla}_\perp\cdot\mathbf{V}_{3\perp}=0, \tag{C12}$$

$$\mathbf{V}_{1\perp}=0,\quad V_{1z}=0,\quad \Theta_1=0\quad\text{at}\quad z=1, \tag{C13}$$

$$\mathbf{V}_\perp 3=0,\quad V_{3z}=0,\quad \Theta_3=s\quad\text{at}\quad \bar{z}=-1; \tag{C14}$$

at z=0,

$$P_1+a_*\frac{\partial P_1}{\partial z}\overline{h}-P_2-a_*\frac{\partial P_2}{\partial z}\overline{h}+\frac{W_0}{a}{}_*\overline{\Delta}_\perp\overline{h}+\mathrm{Ga}\,\delta\overline{h}$$
$$=2a_*\left(\frac{\partial V_{1z}}{\partial z}-\eta^{-1}\frac{\partial V_{2z}}{\partial z}\right)+O(a_*^2), \tag{C15}$$

$$\frac{\partial \mathbf{V}_{1\perp}}{\partial z}-\eta^{-1}\frac{\partial \mathbf{V}_{2\perp}}{\partial z}+a_*\overline{h}\left(\frac{\partial^2\mathbf{V}_{1\perp}}{\partial z^2}-\eta^{-1}\partial^2\mathbf{V}_{2\perp}\partial z^2\right)$$
$$+a_*(\overline{\nabla}V_{1z}-\eta^{-1}\overline{\nabla}V_{2z})-\frac{M_0+ma_*}{P}\overline{\nabla}\Theta_1$$
$$-\frac{M_0}{P}a_*\overline{h}\frac{\partial\overline{\nabla}\Theta_1}{\partial z}-\frac{M_0+ma_*}{P}A_1^0\overline{\nabla h}-\frac{M_0}{P}A_1^1\overline{\nabla h}$$
$$-\frac{M_0}{P}a_*\overline{\nabla h}\frac{\partial\Theta_1}{\partial z}=O(a_*^2), \tag{C16}$$

$$\mathbf{V}_{1\perp}+a_*\overline{h}\frac{\partial\mathbf{V}_{1\perp}}{\partial z}=\mathbf{V}_{2\perp}+a_*\overline{h}\frac{\partial\mathbf{V}_{2\perp}}{\partial z}+O(a_*^2), \tag{C17}$$

$$V_{1z}+a_*\overline{h}\frac{\partial V_{1z}}{\partial z}=V_{2z}+a_*\overline{h}\frac{\partial V_{2z}}{\partial z}+O(a_*^2), \tag{C18}$$

$$a_*\frac{\partial\overline{h}}{\partial\overline{t}}+a_*\mathbf{V}_{1\perp}\cdot\overline{\nabla h}=V_{1z}+a_*h\frac{\partial V_{1z}}{\partial z}+O(a_*^2), \tag{C19}$$

$$\Theta_1+A_1^0\overline{h}+a_*\overline{h}\frac{\partial\Theta_1}{\partial z}=\Theta_2+A_2^0\overline{h}+a_*\overline{h}\frac{\partial\Theta_2}{\partial z}, \tag{C20}$$

$$\frac{\partial\Theta_1}{\partial z}+a_*\overline{h}\frac{\partial^2\Theta_1}{\partial z^2}-\kappa^{-1}\frac{\partial\Theta_2}{\partial z}-\kappa^{-1}a_*\overline{h}\frac{\partial^2\Theta_2}{\partial z^2}=O(a_*^2); \tag{C21}$$

at $z=-a$, $\overline{z}=0$,

$$P_2-P_3-a_*\overline{h}_*\frac{\partial P_3}{\partial\overline{z}}+\mathrm{Ga}\,\delta_*a_*\overline{h}_*+2a_*\eta^{-1}\frac{\partial V_{2z}}{\partial z}$$
$$=O(a_*^2), \tag{C22}$$

$$\eta^{-1}\left(\frac{\partial\mathbf{V}_{2\perp}}{\partial z}+a_*\overline{\nabla}V_{2z}\right)-\eta_*^{-1}\frac{\partial\mathbf{V}_{3\perp}}{\partial\overline{z}}-\frac{\overline{\alpha}M_0}{P}a_*\overline{\nabla}\Theta_3$$
$$=O(a_*^2), \tag{C23}$$

$$\mathbf{V}_{2\perp}=a_*\mathbf{V}_{3\perp}+O(a_*^2), \tag{C24}$$

$$V_{2z}=O(a_*^2), \tag{C25}$$

$$\frac{\partial\overline{h}_*}{\partial\overline{t}}+a_*\mathbf{V}_{3\perp}\cdot\overline{\nabla h}_*=V_{3z}+O(a_*^2), \tag{C26}$$

$$\Theta_2+a_*\overline{h}_*A_2^0=a_*\Theta_3+a_*\overline{h}_*A_3^0+O(a_*^2), \tag{C27}$$

$$\kappa^{-1}\frac{\partial\Theta_2}{\partial z}-\kappa_*^{-1}\frac{\partial\Theta_3}{\partial\overline{z}}-\kappa_*^{-1}a_*\overline{h}_*\frac{\partial^2\Theta_3}{\partial\overline{z}^2}=O(a_*^2), \tag{C28}$$

where

$$\frac{dT_j^0}{dz}=A_j^0+a_*A_j^1+\cdots,$$

$$A_1^0=-\frac{s}{1+\kappa a},\quad A_2^0=-\frac{s\kappa}{1+\kappa a},\quad A_3^0=-\frac{s\kappa_*}{1+\kappa a},$$

$$A_1^1=\frac{s\kappa_*}{(1+\kappa a)^2},\quad A_2^1=\frac{s\kappa\kappa_*}{(1+\kappa a)^2},\quad A_3^1=\frac{s\kappa_*^2}{(1+\kappa a)^2}.$$

We construct the solution in the form (34).

In the zeroth order, we obtain a linear eigenvalue problem that determines the critical Marangoni number (28) and the eigenfunction

$$\Theta_1^{(0)}=\frac{s(\kappa-1)\overline{h}^{(0)}}{(1+\kappa a)^2}(z-1),$$

$$\Theta_2^{(0)}=\frac{s\kappa(\kappa-1)\overline{h}^{(0)}}{(1+\kappa a)^2}(z+a),$$

$$\Theta_3^{(0)}=\frac{s\kappa_*(\kappa-1)\overline{h}^{(0)}}{(1+\kappa a)^2}(\overline{z}+1),$$

$$\mathbf{V}_{1\perp}^{(0)}=\frac{\eta a^2}{1-\eta a^2}\mathrm{Ga}\,\delta\overline{\nabla}_\perp\overline{h}^{(0)}\left(\frac{1}{2}z^2-\frac{2}{3}z+\frac{1}{6}\right),$$

$$V_{1z}^{(0)}=\frac{\eta a^2}{1-\eta a^2}\mathrm{Ga}\,\delta\overline{\Delta}_\perp\overline{h}^{(0)}\left(-\frac{1}{6}z^3+\frac{1}{3}z^2-\frac{1}{6}z\right),$$

$$\mathbf{V}_{2\perp}^{(0)}=\frac{\eta}{1-\eta a^2}\mathrm{Ga}\,\delta\overline{\nabla}_\perp\overline{h}^{(0)}\left(\frac{1}{2}z^2+\frac{2a}{3}z+\frac{a^2}{6}\right),$$

$$V_{2z}^{(0)}=\frac{\eta}{1-\eta a^2}\mathrm{Ga}\,\delta\overline{\Delta}_\perp\overline{h}^{(0)}\left(-\frac{1}{6}z^3-\frac{a}{3}z^2-\frac{a^2}{6}z\right),$$

$$\mathbf{V}_{2\perp}^{(0)}=\frac{\eta_*a}{1-\eta a^2}\mathrm{Ga}\,\delta\overline{\nabla}_\perp\overline{h}^{(0)}\left(-\frac{1}{3}\overline{z}-\frac{1}{3}\right),$$

$$V_{3z}^{(0)}=\frac{\eta_*a}{1-\eta a^2}\mathrm{Ga}\,\delta\overline{\Delta}_\perp\overline{h}^{(0)}\left(\frac{1}{6}\overline{z^2}+\frac{1}{3}\overline{z}+\frac{1}{6}\right),$$

$$P_1^{(0)}=\mathrm{Ga}\,\delta\frac{\eta a^2}{1-\eta a^2}\overline{h}^{(0)},\quad P_2^{(0)}=P_3^{(0)}=\mathrm{Ga}\,\delta\frac{1}{1-\eta a^2}\overline{h}^{(0)}.$$

Also, we obtain the relation (35).

In the first order in $a_*$, we obtain the inhomogeneous linear problem. The solvability condition for this problem gives the relation (36) with

$$m_*=\frac{2s\,\mathrm{Ga}\,\delta P(1+\kappa a)}{3(1-\eta a^2)\kappa(1+a)}\left[\frac{\kappa_*(1+\eta a)(-1+2\kappa+\kappa a)}{\kappa(1+a)}\right.$$
$$\left.+\frac{\eta_*(1+2\eta a+\eta a^2)(1+\kappa a^2)(1+\kappa a)}{\eta(1-\eta a^2)}\right]. \quad \text{(C29)}$$


[1] J. R. A. Pearson, J. Fluid Mech. **4**, 489 (1958).
[2] J. W. Scanlon and L. A. Segel, J. Fluid Mech. **30**, 149 (1967).
[3] Y. Pomeau, Physica D **23**, 3 (1986).
[4] K. A. Smith, J. Fluid Mech. **24**, 401 (1966).
[5] M. Takashima, J. Phys. Soc. Jpn. **50**, 2745 (1981).
[6] S. J. VanHook, M. F. Schatz, W. D. McCormick, J. B. Swift, and H. L. Swinney, Phys. Rev. Lett. **75**, 4397 (1995).
[7] S. J. VanHook, M. F. Schatz, J. B. Swift, W. D. McCormick, and H. L. Swinney, J. Fluid Mech. **345**, 45 (1997).
[8] S. Krishnamoorthy, B. Ramaswamy, and S. W. Joo, Phys. Fluids **7**, 2291 (1995).
[9] S. H. Davis, in *Waves on Fluid Interfaces*, edited by R.E. Meyer (Academic, New York, 1983), p. 291.
[10] S. H. Davis, Annu. Rev. Fluid Mech. **19**, 403 (1987).
[11] T. Funada, J. Phys. Soc. Jpn. **56**, 2031 (1987).
[12] V. V. Pukhnachev, *Thermocapillary Convection at Reduced Gravitation* (Institute of Hydrodynamics SB AS USSR, Novosibirsk, 1987).
[13] I. B. Simanovskii and A. A. Nepomnyashchy, *Convective Instabilities in Systems with Interface* (Gordon and Breach, London, 1993).
[14] A. A. Nepomnyashchy and I. B. Simanovskii, Prikl. Mat. Mekh. **54**, 593 (1990) [J. Appl. Math. Mech. **54**, 490 (1990)].
[15] T. Funada, J. Phys. Soc. Jpn. **55**, 2191 (1986).
[16] S. Wahal and A. Bose, Phys. Fluids **31**, 3502 (1988).
[17] Ph. Georis, M. Hennenberg, J.-C. Legros, A. A. Nepomnyashchy, I. B. Simanovskii, and I. I. Wertgeim, in *Hydrodynamics and Heat/Mass Transfer in Microgravity*, edited by V. S. Avduevsky *et al.* (Gordon and Breach, London, 1992), pp. 105–109.
[18] I. B. Simanovskii, Ph. Georis, M. Hennenberg, S. Van Vaerenberg, I. I. Wertgeim, and J.-C. Legros, *Proceedings VIII European Symposium on Materials and Fluid Sciences in Microgravity* (European Space Agency, Paris, 1992), pp. 729–734.
[19] Q. S. Liu and B. Roux, *Proceedings VIII European Symposium on Materials and Fluid Sciences in Microgravity* (Ref. [18]), pp. 735–740.
[20] Ph. Georis, M. Hennenberg, I. B. Simanovskii, A. A. Nepomnyashchy, I. I. Wertgeim, and J.-C. Legros, Phys. Fluids A **5**, 1575 (1993).
[21] A. Oron, R. J. Deissler, and J. C. Duh, Eur. J. Mech. B/Fluids **14**, 737 (1995).
[22] Ph. Georis and J.-C. Legros, in *Materials and Fluids under Low Gravity*, edited by L. Ratke, H. Walter, and B. Feuerbacher (Springer, Berlin, 1996), pp. 293–311.
[23] A. A. Nepomnyashchy and I. B. Simanovskii, Q. J. Mech. Appl. Math. **50**, 149 (1997).
[24] V. Kats-Demyanets, A. Oron, and A. Nepomnyashchy, Eur. J. Mech. B/Fluids **16**, 49 (1997).
[25] C. C. Chen and C. J. Lee, J. Membr. Sci. **20**, 1 (1984).
[26] H. Groothuis and F. G. Zuiderweg, Chem. Eng. Sci. **12**, 288 (1960).
[27] G. I. Sivashinsky, Physica D **8**, 243 (1983).
[28] J. S. Langer, Rev. Mod. Phys. **52**, 1 (1980).
[29] K. Kawasaki and T. Ohta, Physica A **116**, 573 (1982).
[30] L. M. Pismen, Phys. Rev. A **38**, 2564 (1988).
[31] B. Van der Pol, Philos. Mag. **2**, 978 (1926).